Decoherence of Quantum-Enhanced Timing Accuracy

Mankei Tsang

Department of Electrical Engineering, California Institute of Technology, Pasadena, CA 91125

(Dated: February 5, 2008)

Quantum enhancement of optical pulse timing accuracy is investigated in the Heisenberg picture. Effects of optical loss, group-velocity dispersion, and Kerr nonlinearity on the position and momentum of an optical pulse are studied via Heisenberg equations of motion. Using the developed formalism, the impact of decoherence by optical loss on the use of adiabatic soliton control for beating the timing standard quantum limit [Tsang, Phys. Rev. Lett. **97**, 023902 (2006)] is analyzed theoretically and numerically. The analysis shows that an appreciable enhancement can be achieved using current technology, despite an increase in timing jitter mainly due to the Gordon-Haus effect. The decoherence effect of optical loss on the transmission of quantum-enhanced timing information is also studied, in order to identify situations in which the enhancement is able to survive.

I. INTRODUCTION

It has been suggested that the use of correlated photons is able to enhance the position accuracy of an optical pulse beyond the standard quantum limit, and the enhancement can be useful for positioning and clock synchronization applications [1]. Generation of two photons with the requisite correlation has been demonstrated experimentally by Kuzucu *et al.* [2], but in practice it is more desirable to produce as many correlated photons as possible in order to obtain a higher accuracy. To achieve quantum enhancement for a large number of photons, a scheme of adiabatically manipulating optical fiber solitons has recently been proposed [3], opening up a viable route of applying quantum enhancement to practical situations. The analysis in Ref. [3] assumes that the optical fibers are lossless, so the Heisenberg limit [4] can be reached in principle. In reality, however, the quantum noise associated with optical loss increases the soliton timing jitter and limits the achievable enhancement. Compared with the use of solitons for quadrature squeezing [5], the adiabatic soliton control scheme potentially suffers more from decoherence, because the soliton must propagate for a longer distance to satisfy the adiabatic approximation. The effect of loss on a similar scheme of soliton momentum squeezing has been studied by Fini and Hagelstein [6], although they did not study the timing jitter evolution relevant to the scheme in Ref. [3], and did not take into account possible departure from the adiabatic approximation.

In this paper, the decoherence effect of optical loss on the timing accuracy enhancement scheme proposed in Ref. [3] is investigated in depth, in order to evaluate the performance of the scheme in practice. Instead of approaching the problem in the Schrödinger picture like prior work [1, 3, 6, 7], this paper primarily utilizes Heisenberg equations of motion, since they are able to account for dissipation and fluctuation in a more elegant way. For simplicity, scalar solitons, as opposed to vector solitons studied in Ref. [3], are considered here. The theoretical and numerical analyses show that, despite an increase in timing jitter due to quantum noise and deviation from the adiabatic approximation, an appreciable enhancement can still be achieved using a realistic setup.

The developed formalism is also used to study the propagation of an optical pulse with quantum-enhanced timing accuracy in a lossy, dispersive, and nonlinear medium, such as an optical fiber, in order to identify situations in which the enhancement can still survive. The effect of loss on many correlated photons sent in as many channels has been investigated by Giovannetti *et al.* [1], but their analysis focuses on a relatively small number of correlated photons and does not include the effects of dispersion and nonlinearity.

This paper is organized as follows: Section II defines the general theoretical framework, and derives the standard quantum limits and Heisenberg limits on the variances of the pulse position and momentum operators. Section III studies the evolution of such operators in the presence of loss, group-velocity dispersion, and Kerr nonlinearity, and determines the effect of dissipation and fluctuation on the position and momentum uncertainties. Section IV investigates theoretically and numerically the impact of optical loss on the adiabatic soliton control scheme using realistic parameters, while Sec. V studies the decoherence effect on the transmission of the quantum-enhanced timing information in various linear and nonlinear systems.

II. THEORETICAL FRAMEWORK

A. Definition of pulse position and momentum operators

The positive-frequency electric field of a waveguide mode at a certain longitudinal position can be defined as [8]

$$\hat{E}^{(+)}(t) = i \int_0^\infty d\omega \left(\frac{\hbar\omega\eta}{4\pi\varepsilon_0 c n^2 S} \right)^{1/2} \hat{c}(\omega) e^{-i\omega t}, \qquad (1)$$

where n is the refractive index, η is the real part of n, S is the transverse area of the waveguide mode, and $\hat{c}(\omega)$ is the photon annihilation operator. The annihilation operator is related to the corresponding creation operator via the commutator [8],

$$[\hat{c}(\omega), \hat{c}^\dagger(\omega')] = \delta(\omega - \omega'). \qquad (2)$$

For a pulse with a slowly-varying envelope compared with the optical frequency, the coefficient in front of the annihilation operator can be assumed to be independent of frequency and

can be evaluated at the carrier frequency ω_0, so that the electric field is proportional to the temporal envelope annihilation operator $\hat{A}(t)$,

$$\hat{E}^{(+)}(t) \propto \hat{A}(t)e^{-i\omega_0 t}, \tag{3}$$

$$\hat{A}(t) \equiv \frac{1}{\sqrt{2\pi}} \int d\omega\, \hat{a}(\omega)e^{-i\omega t}, \tag{4}$$

$$\hat{a}(\omega) \equiv \hat{c}(\omega + \omega_0). \tag{5}$$

The temporal envelope operator $\hat{A}(t)$ and the spectral operator $\hat{a}(\omega)$ evidently also satisfy the following commutation relations with their corresponding creation operators,

$$[\hat{A}(t), \hat{A}^\dagger(t')] = \delta(t - t'), \tag{6}$$

$$[\hat{a}(\omega), \hat{a}^\dagger(\omega')] = \delta(\omega - \omega'). \tag{7}$$

The total photon number operator can be defined as

$$\hat{N} \equiv \int dt\, \hat{A}^\dagger(t)\hat{A}(t), \tag{8}$$

and the pulse center position operator as [9]

$$\hat{T} \equiv \frac{1}{N} \int dt\, t\hat{A}^\dagger(t)\hat{A}(t), \tag{9}$$

where

$$N \equiv \langle \hat{N} \rangle \tag{10}$$

is the average photon number. This definition uses $1/N$ as the normalization coefficient, instead of the inverse photon number operator $\hat{N}^{-1}$ used by Lai and Haus [10], in order to express the position operator in terms of normally ordered optical field operators that are easier to handle, as well as to avoid the potential problem of applying $\hat{N}^{-1}$ on the vacuum state. As long as the photon-number fluctuation is small, the position operator naturally corresponds to the measurement of the center position of the pulse intensity profile. An average longitudinal momentum operator can be similarly defined,

$$\hat{\Omega} \equiv \frac{1}{N} \int d\omega\, \omega\hat{a}^\dagger(\omega)\hat{a}(\omega)$$
$$= \frac{1}{N} \int dt\, \hat{A}^\dagger(t) \left(i\frac{\partial}{\partial t}\right) \hat{A}(t). \tag{11}$$

If the quantum state is close to a large-photon-number coherent state, $\hat{A}$ can be approximated as $\langle \hat{A} \rangle + \delta\hat{A}$, with $O(\delta\hat{A}) \ll O(\hat{A})$. Equations (9) and (11) then become the approximate position and momentum operators defined by Haus and Lai for solitons in a linearized approach [11]. The linearized expressions also describe how they can be accurately measured in practice using balanced homodyne detection [11].

For simplicity, we shall hereafter assume that $\langle \hat{T} \rangle = 0$ and $\langle \hat{\Omega} \rangle = 0$ [9]. In the systems considered in this paper, these two quantities remain constant throughout propagation, if t is regarded as the retarded time in the moving frame of the optical pulse.

The commutator between the position and momentum operators is

$$[\hat{T}, \hat{\Omega}] = \frac{i\hat{N}}{N^2}. \tag{12}$$

By the Heisenberg uncertainty principle,

$$\langle \hat{T}^2 \rangle \langle \hat{\Omega}^2 \rangle \geq \left(\frac{1}{2i}\langle[\hat{T}, \hat{\Omega}]\rangle\right)^2 = \frac{1}{4N^2}. \tag{13}$$

B. Derivation of standard quantum limits

The standard quantum limits and Heisenberg limits on $\langle \hat{\Omega}^2 \rangle$ and $\langle \hat{T}^2 \rangle$ should be expressed in terms of the pulse width Δt, defined as

$$\Delta t \equiv \left\langle \frac{1}{N} \int dt\, t^2 \hat{A}^\dagger(t)\hat{A}(t) \right\rangle^{1/2}, \tag{14}$$

and the bandwidth $\Delta\omega$,

$$\Delta\omega \equiv \left\langle \frac{1}{N} \int d\omega\, \omega^2 \hat{a}^\dagger(\omega)\hat{a}(\omega) \right\rangle^{1/2}$$
$$= \left\langle \frac{1}{N} \int dt\, \hat{A}^\dagger(t) \left(-\frac{\partial^2}{\partial t^2}\right) \hat{A}(t) \right\rangle^{1/2}. \tag{15}$$

To calculate the standard quantum limit on the position uncertainty, consider the expansion

$$\langle \hat{\Omega}^2 \rangle = \frac{1}{N^2} \left\langle \int d\omega\, \omega\hat{a}^\dagger\hat{a} \int d\omega'\, \omega'\hat{a}'^\dagger\hat{a}' \right\rangle, \tag{16}$$

where we have written $\hat{a} = \hat{a}(\omega)$ and $\hat{a}' = \hat{a}(\omega')$ as shorthands. Rearranging the operators,

$$\langle \hat{\Omega}^2 \rangle = \frac{1}{N} \left\langle \frac{1}{N} \int d\omega\, \omega^2 \hat{a}^\dagger\hat{a} \right\rangle$$
$$+ \frac{1}{N^2} \left\langle \int d\omega \int d\omega'\, \omega\omega'\hat{a}^\dagger\hat{a}'^\dagger\hat{a}\hat{a}' \right\rangle. \tag{17}$$

The first term on the right-hand side of Eq. (17) is proportional to $\Delta\omega^2$, while the second term contains a normally ordered cross-spectral density. To derive the standard quantum limit, we shall assume that the cross-spectral density satisfies the factorization condition:

$$\langle \hat{a}^\dagger\hat{a}'^\dagger\hat{a}\hat{a}' \rangle \propto \langle \hat{a}^\dagger\hat{a} \rangle \langle \hat{a}'^\dagger\hat{a}' \rangle. \tag{18}$$

This condition is always satisfied by any pure or mixed state with only one excited optical mode, such as a coherent state [12, 13]. The second term on the right-hand side of Eq. (17) becomes

$$\frac{1}{N^2} \int d\omega \int d\omega'\, \omega\omega' \langle \hat{a}^\dagger\hat{a}'^\dagger\hat{a}\hat{a}' \rangle \propto \langle \hat{\Omega} \rangle^2, \tag{19}$$

which is assumed to be zero, as per the convention of this paper. Thus, the variance of $\hat{\Omega}$ is

$$\langle \hat{\Omega}^2 \rangle_{\text{coh}} = \frac{\Delta \omega^2}{N}, \tag{20}$$

where the subscript "coh" denotes statistics of coherent fields [12, 13] given by Eq. (18). By virtue of the Heisenberg uncertainty principle given by Eq. (13), the standard quantum limit on the position variance is hence

$$\langle \hat{T}^2 \rangle \geq \langle \hat{T}^2 \rangle_{\text{SQL}} = \frac{1}{4N^2 \langle \hat{\Omega}^2 \rangle_{\text{coh}}} = \frac{1}{4N\Delta \omega^2}. \tag{21}$$

This limit is applicable to any pure or mixed state, and is consistent with the one suggested by Giovannetti *et al.* for Fock states [1]. A very similar derivation of the limit for Fock states and coherent states is also performed by Vaughan *et al.* [9].

Owing to Fourier duality of position and momentum in the slowly-varying envelope regime, the standard quantum limit on the momentum can be derived in the same way. The variance of $\hat{T}$, assuming coherent-field statistics, is

$$\langle \hat{T}^2 \rangle_{\text{coh}} = \frac{\Delta t^2}{N}, \tag{22}$$

and the standard quantum limit on the momentum variance is

$$\langle \hat{\Omega}^2 \rangle_{\text{SQL}} = \frac{1}{4N^2 \langle \hat{T}^2 \rangle_{\text{coh}}} = \frac{1}{4N\Delta t^2}. \tag{23}$$

C. Derivation of Heisenberg limits

To derive the Heisenberg limit on the position uncertainty, one needs an absolute upper bound on the momentum uncertainty $\langle \hat{\Omega}^2 \rangle$. Consider the following non-negative quantity proportional to the coherence bandwidth squared,

$$\int d\omega \int d\omega' \, (\omega - \omega')^2 \, \langle \hat{a}^\dagger \hat{a}'^\dagger \hat{a} \hat{a}' \rangle \geq 0. \tag{24}$$

This quantity is non-negative because $(\omega - \omega')^2$ is non-negative and $\langle \hat{a}^\dagger \hat{a}'^\dagger \hat{a} \hat{a}' \rangle$ is also non-negative [13]. It can be rewritten as

$$\int d\omega \int d\omega' \, (\omega - \omega')^2 \, \langle \hat{a}^\dagger \hat{a}'^\dagger \hat{a} \hat{a}' \rangle$$
$$= \int d\omega \int d\omega' \, (\omega - \omega')^2 \, \langle \hat{a}^\dagger \hat{a} \hat{a}'^\dagger \hat{a}' \rangle, \tag{25}$$

and expanded as

$$\left\langle \int d\omega \int d\omega' \, (\omega^2 + \omega'^2 - 2\omega\omega') \hat{a}^\dagger \hat{a} \hat{a}'^\dagger \hat{a}' \right\rangle \geq 0,$$
$$2 \left\langle \hat{N} \int d\omega \, \omega^2 \hat{a}^\dagger \hat{a} \right\rangle - 2N^2 \langle \hat{\Omega}^2 \rangle \geq 0. \tag{26}$$

Here we shall approximate $\hat{N}$ with N, and neglect any photon-number fluctuation. This approximation is exact for Fock

states, and acceptable for any quantum state with a small photon-number fluctuation, such as a large-photon-number coherent state. We then obtain the following approximate inequality,

$$\langle \hat{\Omega}^2 \rangle \leq \Delta \omega^2. \tag{27}$$

With the Heisenberg uncertainty principle given by Eq. (13) and the upper bound on $\langle \hat{\Omega}^2 \rangle$ given by Eq. (27), one can then obtain the Heisenberg limit on the uncertainty of $\hat{T}$:

$$\langle \hat{T}^2 \rangle \geq \langle \hat{T}^2 \rangle_{\text{H}} = \frac{1}{4N^2\Delta \omega^2}. \tag{28}$$

Equation (28) is again consistent with the Heisenberg limit suggested by Giovannetti *et al.* [1], although the derivation here shows that it is not only valid for Fock states but also correct to the first order for any quantum state with a small photon-number fluctuation.

The Heisenberg limit on $\langle \hat{\Omega}^2 \rangle$ is similar,

$$\langle \hat{\Omega}^2 \rangle_{\text{H}} = \frac{1}{4N^2\Delta t^2}. \tag{29}$$

A more exact derivation of the Heisenberg limits is given in Appendix A, where the inverse photon-number operator $\hat{N}^{-1}$ is used instead of $1/N$ in the definitions of $\hat{T}$, $\hat{\Omega}$, $\Delta\omega$, and Δt. The difference between the approximate Heisenberg limits derived here and the exact Heisenberg limits in Appendix A is negligible for small photon-number fluctuations.

III. OPTICAL PULSE PROPAGATION IN THE HEISENBERG PICTURE

The classical nonlinear Schrödinger equation that describes the propagation of pulses in a lossy, dispersive, and nonlinear medium, such as an optical fiber, is given by [14]

$$i\frac{\partial A}{\partial z} = \frac{\beta}{2} \frac{\partial^2 A}{\partial t^2} - \kappa |A|^2 A - \frac{i\alpha}{2} A, \tag{30}$$

where t is the retarded time coordinate in the frame of the moving pulse, β is the group-velocity dispersion coefficient, κ is the normalized Kerr coefficient, and α is the loss coefficient, all of which may depend on z. The phenomenological quantized version that preserves the commutator between $\hat{A}$ and $\hat{A}^\dagger$ is [5]

$$i\frac{\partial \hat{A}}{\partial z} = \frac{\beta}{2} \frac{\partial^2 \hat{A}}{\partial t^2} - \kappa \hat{A}^\dagger \hat{A} \hat{A} - \frac{i\alpha}{2} \hat{A} + i\hat{s}. \tag{31}$$

$\hat{A} \equiv \hat{A}(z,t)$ is the pulse envelope annihilation operator in the Heisenberg picture, and $\hat{s}$ is the Langevin noise operator, satisfying the commutation relation

$$[\hat{s}(z,t), \hat{s}^\dagger(z',t')] = \alpha\delta(z-z')\delta(t-t'). \tag{32}$$

Rewriting the position and momentum operators in Eqs. (9) and (11) in the Heisenberg picture as $\hat{T}(z)$ and $\hat{\Omega}(z)$ in terms of

$\hat{A}(z,t)$, differentiating them with respect to z, and using Eq. (31), their equations of motion can be derived,

$$\frac{d\hat{T}(z)}{dz} = \beta(z)\hat{\Omega}(z) + \hat{S}_T(z), \qquad (33)$$

$$\frac{d\hat{\Omega}(z)}{dz} = \hat{S}_\Omega(z), \qquad (34)$$

where $\hat{S}_T$ and $\hat{S}_\Omega$ are position and momentum noise operators defined as

$$\hat{S}_T(z) \equiv \frac{1}{N(z)} \int dt\, t\hat{s}^\dagger(z,t)\hat{A}(z,t) + \text{H. c.}, \qquad (35)$$

$$\hat{S}_\Omega(z) \equiv \frac{1}{N(z)} \int dt\, \hat{s}^\dagger(z,t)\left(i\frac{\partial}{\partial t}\right)\hat{A}(z,t) + \text{H. c.}, \qquad (36)$$

and H. c. denotes Hermitian conjugate. If the noise reservoir is assumed to be in the vacuum state, the noise operators have the following statistical properties, as shown in Appendix B,

$$\langle \hat{S}_T(z)\rangle = 0, \ \langle \hat{S}_\Omega(z)\rangle = 0, \qquad (37)$$

$$\langle \hat{S}_T(z)\hat{S}_T(z')\rangle = \frac{\alpha(z)\Delta t^2(z)}{N(z)}\delta(z-z'), \quad (38)$$

$$\langle \hat{S}_\Omega(z)\hat{S}_\Omega(z')\rangle = \frac{\alpha(z)\Delta\omega^2(z)}{N(z)}\delta(z-z'), \quad (39)$$

$$\langle \hat{S}_T(z)\hat{S}_\Omega(z') + \hat{S}_\Omega(z)\hat{S}_T(z')\rangle = \frac{\alpha(z)C(z)}{N(z)}\delta(z-z'), \qquad (40)$$

where $C(z)$ is the pulse chirp factor, defined as

$$C(z) \equiv \left\langle \frac{1}{N(z)}\int dt\, \hat{A}^\dagger(z,t)\left[t\left(i\frac{\partial}{\partial t}\right) + \left(i\frac{\partial}{\partial t}\right)t\right]\hat{A}(z,t)\right\rangle. \qquad (41)$$

The average position $\langle \hat{T}(z)\rangle$ and average momentum $\langle \hat{\Omega}(z)\rangle$ are constant and assumed to be zero throughout propagation. The variance of $\hat{\Omega}$ is then

$$\langle \hat{\Omega}^2(z)\rangle = \langle \hat{\Omega}^2(0)\rangle + \int_0^z dz'\frac{\alpha(z')\Delta\omega^2(z')}{N(z')}, \qquad (42)$$

while the variance of $\hat{T}$ is more complicated due to the presence of dispersion,

$$\langle \hat{T}^2(z)\rangle = \langle \hat{T}^2(0)\rangle + \langle \hat{T}(0)\hat{\Omega}(0) + \hat{\Omega}(0)\hat{T}(0)\rangle \int_0^z dz'\beta(z')$$

$$+ \langle \hat{\Omega}^2(0)\rangle\left[\int_0^z dz'\beta(z')\right]^2$$

$$+ \int_0^z dz'\frac{\alpha(z')\Delta t^2(z')}{N(z')}$$

$$+ \int_0^z dz'\beta(z')\int_0^{z'} dz''\frac{\alpha(z'')C(z'')}{N(z'')}$$

$$+ 2\int_0^z dz'\beta(z')\int_0^{z'} dz''\beta(z'')$$

$$\times \int_0^{z''} dz'''\frac{\alpha(z''')\Delta\omega^2(z''')}{N(z''')}. \qquad (43)$$

Equation (43) is the central result of this paper. It is similar to that derived by Haus for optical solitons using a linearized approach [15], but Eq. (43) is valid for arbitrary loss, arbitrary dispersion profile $\beta(z)$, and arbitrary evolution of pulse width $\Delta t(z)$, chirp $C(z)$, and bandwidth $\Delta\omega(z)$, so that it is able to describe the effect of loss on the quantum enhancement scheme proposed in Ref. [3]. The first term on the right-hand side of Eq. (43) is the initial quantum fluctuation, while the second and third term on the right-hand side describe the quantum dispersion effect [16]. In an ideal scenario described in Ref. [3], $\langle \hat{T}^2(z)\rangle$ remains constant if the net dispersion $\int_0^z dz'\beta(z')$ is zero and quantum dispersion is compensated. With loss, however, noise introduces a diffusive jitter given by the fourth term on the right-hand side of Eq. (43),

$$\langle \hat{T}^2(z)\rangle_{\text{D}} \equiv \int_0^z dz'\frac{\alpha(z')\Delta t^2(z')}{N(z')}, \qquad (44)$$

a less well-known chirp-induced jitter given by the fifth term,

$$\langle \hat{T}^2(z)\rangle_{\text{C}} \equiv \int_0^z dz'\beta(z')\int_0^{z'} dz''\frac{\alpha(z'')C(z'')}{N(z'')}, \qquad (45)$$

and also the Gordon-Haus timing jitter [17] given by the sixth term,

$$\langle \hat{T}^2(z)\rangle_{\text{GH}} \equiv 2\int_0^z dz'\beta(z')\int_0^{z'} dz''\beta(z'')$$

$$\times \int_0^{z''} dz'''\frac{\alpha(z''')\Delta\omega^2(z''')}{N(z''')}. \qquad (46)$$

In most cases considered here, $N \gg 1$, $\langle \hat{T}^2\rangle \ll \Delta t^2$, and $\langle \hat{\Omega}^2\rangle \ll \Delta\omega^2$, so one can use the classical nonlinear Schrödinger equation, Eq. (30), to predict the evolution of $\Delta t(z)$, $C(z)$, and $\Delta\omega(z)$ accurately. The evolution of $\langle \hat{T}^2(z)\rangle$ can subsequently be calculated analytically or numerically using Eq. (43) and the classical evolution of $\Delta t(z)$, $C(z)$, and $\Delta\omega(z)$, analogous to the linearized approach [11, 15].

It is worth noting that the chirp-induced jitter, Eq. (45), depends on the cross-correlation between the position and momentum noise in Eq. (40), so it can be positive as well as negative, but the sum of the three sources of jitter must obviously remain positive.

IV. EFFECT OF LOSS ON ADIABATIC SOLITON CONTROL

A. Review of the ideal case

Consider the scheme proposed in Ref. [3] and depicted in Fig. 1. Assume that the dispersion coefficient of the first fiber $\beta(z)$ is negative and its magnitude increases along the fiber slowly compared with the soliton period. The classical soliton solution of Eq. (30), assuming adiabatic change in parameters
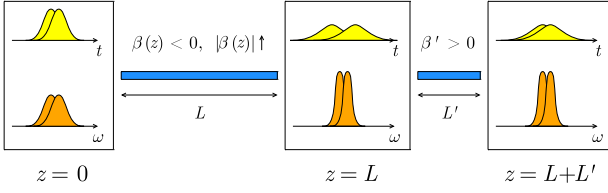
FIG. 1: (Color online) Schematic (not-to-scale) of the adiabatic soliton control scheme. An optical pulse is coupled into a dispersion-increasing fiber of length L with a negative dispersion coefficient β, followed by a much shorter dispersion-compensating fiber of length L' with a positive dispersion coefficient β'.

$\beta(z)$ and $N(z)$, is [18]

$$A(z,t) = A_0(z)\,\text{sech}\left[\frac{t}{\tau(z)}\right]\exp\left[\frac{i\kappa}{2}\int_0^z dz' |A_0(z')|^2\right], \quad (47)$$

$$A_0(z) = \sqrt{\frac{N(z)}{2\tau(z)}}, \ \tau(z) = \frac{2|\beta(z)|}{\kappa N(z)}. \quad (48)$$

The adiabatic approximation is satisfied when

$$\left|\frac{\beta(z)}{d\beta(z)/dz}\right| \ll \Lambda, \ \left|\frac{N(z)}{dN(z)/dz}\right| = \frac{1}{\alpha} \ll \Lambda, \quad (49)$$

where Λ is the soliton period,

$$\Lambda(z) \equiv \frac{\pi}{2}\frac{\tau^2(z)}{|\beta(z)|}. \quad (50)$$

The root-mean-square pulse width $\Delta t(z)$ and bandwidth $\Delta\omega(z)$ then become

$$\Delta t(z) = \frac{\pi}{2\sqrt{3}}\tau(z) = \frac{\pi}{\sqrt{3}}\frac{|\beta(z)|}{\kappa N(z)}, \quad (51)$$

$$\Delta\omega(z) = \frac{1}{\sqrt{3}\tau(z)} = \frac{1}{2\sqrt{3}}\frac{\kappa N(z)}{|\beta(z)|}. \quad (52)$$

The bandwidth $\Delta\omega(z)$ is thus reduced in the first fiber. If the second fiber has a positive dispersion coefficient β' so that the net dispersion is zero ($\int_0^L dz\beta(z) + \beta'L' = 0$), the quantum dispersion effect given by the second and third term on the right-hand side of Eq. (43) can be eliminated. Furthermore, if β' has a very large magnitude compared with $\beta(z)$ so that the second fiber can be very short compared with the first fiber, the effective nonlinearity experienced by the pulse in the second fiber can be neglected, and $\Delta\omega(z)$ remains essentially constant in the second fiber. In the lossless case, the final timing jitter $\langle \hat{T}^2(L+L')\rangle$ is therefore the same as the input $\langle \hat{T}^2(0)\rangle$, but $\Delta\omega(L+L')$ has been reduced and the standard quantum limit on $\langle \hat{T}^2(L+L')\rangle$, Eq. (21), is raised. Provided that the initial timing jitter of a laser pulse obeys the coherent-field statistics given by Eq. (22), the final timing jitter is

$$\langle \hat{T}^2(L+L')\rangle = \langle \hat{T}^2(0)\rangle = \frac{\Delta t^2(0)}{N} = \frac{\pi^2}{3}\frac{\beta^2(0)}{\kappa^2 N^3}, \quad (53)$$

while the final standard quantum limit is

$$\langle \hat{T}^2(L+L')\rangle_{\text{SQL}} = \frac{1}{4N\Delta\omega^2(L+L')} = \frac{3\beta^2(L)}{\kappa^2 N^3}. \quad (54)$$

A timing jitter squeezing ratio, analogous to the squeezing ratio defined by Haus and Lai [11], can be defined as

$$R = \frac{\langle \hat{T}^2(L+L')\rangle}{\langle \hat{T}^2(L+L')\rangle_{\text{SQL}}} = \frac{\pi^2}{9}\frac{\beta^2(0)}{\beta^2(L)}. \quad (55)$$

The factor of $\pi^2/9$ arises because the initial jitter for a sech pulse shape is slightly higher than the standard quantum limit given by Eq. (21) in terms of the bandwidth. As long as $\beta(L)$ at the end of the first fiber is significantly larger than the initial value, the timing jitter becomes lower than the raised standard quantum limit, R becomes smaller than 1, and quantum enhancement of position accuracy is accomplished. This semiclassical analysis is valid in all practical cases, where $N \gg 1$, $R \gg 1/N$, $\langle \hat{T}^2\rangle \ll \Delta t^2$, $\langle \hat{\Omega}^2\rangle \ll \Delta\omega^2$, and is consistent with the analysis of exact quantum soliton theory in Ref. [3]. R is related to the quantum enhancement factor γ defined in Ref. [3] by $R = 1/\gamma^2$. The semiclassical analysis is no longer valid when R is close to the Heisenberg limit $1/N$, but as the next sections will show, owing to decoherence effects, it is extremely difficult for the enhancement to get anywhere close to the Heisenberg limit.

B. Numerical analysis of a realistic case

To investigate the impact of noise and the validity of the adiabatic approximation in practice, a numerical evaluation of $\Delta t(z)$, $C(z)$, $\Delta\omega(z)$, and $\langle \hat{T}^2(z)\rangle$, using Eqs. (30) and (43) and realistic parameters, is necessary. $\beta(z)$ is assumed to have the following profile used in Ref. [19],

$$\beta(z) = \frac{-12.75 \text{ ps}^2/\text{km}}{1 + (L-z)/L_\beta}. \quad (56)$$

$L_\beta = 1$ km is used here instead of the $L_\beta = 1/12$ km used in Ref. [19], in order to satisfy the adiabatic approximation for a longer pulse in this example. Other fiber parameters are $\alpha = 0.4$ dB/km, $n_2 = 2.6 \times 10^{-16}$ cm^2/W, $A_{\text{eff}} = 30$ μm^2 [19], $\lambda_0 = 1550$ nm, $\omega_0 = 2\pi c/\lambda_0$, so that $\kappa = \hbar\omega_0(\omega_0 n_2/cA_{\text{eff}})$. L is assumed to be 2 km. A dispersion-compensating fiber with $\beta' = 127.5$ ps^2/km, $\alpha = 0.4$ dB/km, $n_2 = 2.7 \times 10^{-16}$ cm^2/W, $A_{\text{eff}} = 15$ μm^2 [20], and $L' = 110$ m is used in the numerical analysis as the second fiber. The classical nonlinear Schrödinger equation, Eq. (30), is numerically solved using the Fourier split-step method [14]. An initial sech soliton pulse with $\tau(0) = 1$ ps, $N(0) = 1.9 \times 10^7$, and an initial energy of 2.4 pJ is assumed.

Figure 2 plots the numerical evolution of pulse intensity and spectrum in the two fibers. As expected, the bandwidth is narrowed in the first fiber and remains approximately constant in the second ($z > 2000$ m), owing to the latter's relative short length. Figure 3 plots the evolution of pulse width $\Delta t(z)$, chirp
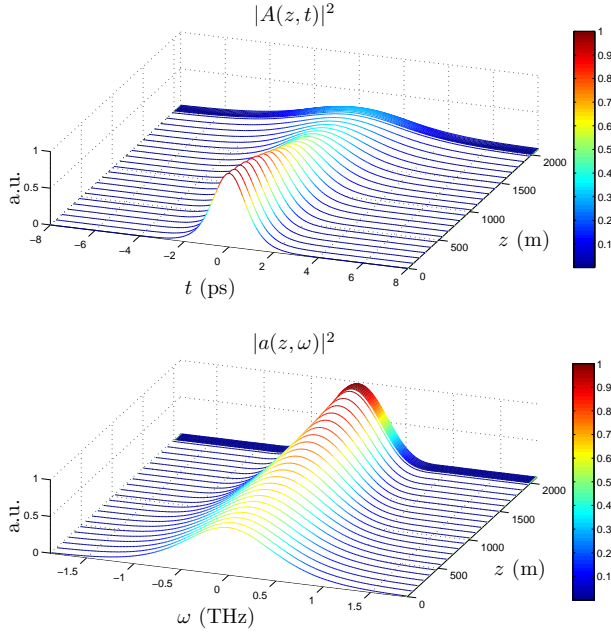
FIG. 2: (Color online) Numerical evolution of pulse intensity (top) and spectrum (bottom). The denser plots for $z > 2000$ m indicate pulse propagation in the second fiber. The color codes are in the same arbitrary units as the heights of the plots.
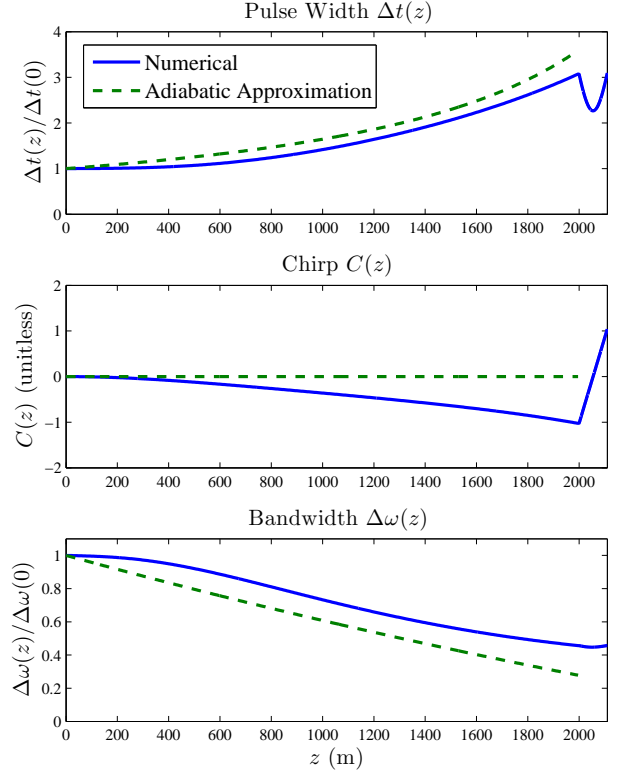

FIG. 3: (Color online) Evolution of pulse width $\Delta t(z)$ (top), chirp $C(z)$ (center), and bandwidth $\Delta\omega$ (bottom), compared with the adiabatic approximation (dash). Plots of Δt and $\Delta\omega$ are normalized with respect to their initial values, respectively.

$C(z)$, and bandwidth $\Delta\omega(z)$, compared with the adiabatic approximation, Eqs. (51) and (52). The adiabatic approximation is evidently not exact, and the pulse acquires a chirp due to excess dispersion in the first fiber, leading to slight refocusing in the second fiber. The bandwidth is reduced by a factor of 2.2, as opposed to the ideal factor of 3.6.

Figure 4 plots the evolution of the diffusive jitter given by Eq. (44), the chirp-induced jitter given by Eq. (45), and the Gordon-Haus jitter given by Eq. (46). It can be seen that although the Gordon-Haus jitter increases much more quickly than the other jitter components in the first fiber, the former drops abruptly in the second fiber ($z > 2000$ m) due to the opposite dispersion. This kind of Gordon-Haus jitter reduction by dispersion management is well known [21]. The chirp-induced jitter component drops below zero in the second fiber, but as noted before, the total noise jitter remains positive. The final jitter values are numerically determined to be $\left\langle \hat{T}^2(L+L') \right\rangle_{\rm D} = 0.71 \left\langle \hat{T}^2(0) \right\rangle$, $\left\langle \hat{T}^2(L+L') \right\rangle_{\rm C} = -0.93 \left\langle \hat{T}^2(0) \right\rangle$, and $\left\langle \hat{T}^2(L+L') \right\rangle_{\rm GH} = 1.42 \left\langle \hat{T}^2(0) \right\rangle$, resulting in a total jitter of

$$\begin{aligned}
\left\langle \hat{T}^2(L+L') \right\rangle &= \left\langle \hat{T}^2(0) \right\rangle + \left\langle \hat{T}^2(L+L') \right\rangle_{\rm D} \\
&\quad + \left\langle \hat{T}^2(L+L') \right\rangle_{C} + \left\langle \hat{T}^2(L+L') \right\rangle_{\rm GH} \\
&= 2.19 \left\langle \hat{T}^2(0) \right\rangle.
\end{aligned} \tag{57}$$

The final squeezing ratio is hence

$$\begin{aligned}
R &= \frac{\left\langle \hat{T}^2(L+L') \right\rangle}{\left\langle \hat{T}^2(L+L') \right\rangle_{\rm SQL}} \\
&= \frac{\pi^2}{9} \frac{\left\langle \hat{T}^2(L+L') \right\rangle}{\left\langle \hat{T}^2(0) \right\rangle} \frac{N(L+L')}{N(0)} \frac{\Delta\omega^2(L+L')}{\Delta\omega^2(0)} \\
&= 0.42 = -3.8 \text{ dB}.
\end{aligned} \tag{58}$$

Despite taking into account the increased timing jitter and the non-ideal bandwidth narrowing, a squeezing ratio of -3.8 dB is predicted by the numerical analysis, suggesting that one should be able to observe the quantum enhancement experimentally using current technology.

C. Potential improvements

As shown in the previous section, the Gordon-Haus effect contributes the largest amount of noise in the soliton control scheme, despite its partial reduction by dispersion management. Its magnitude at the end of the first fiber can be estimated roughly as

$$\frac{\left\langle \hat{T}^2(L) \right\rangle_{\rm GH}}{\left\langle \hat{T}^2(L) \right\rangle_{\rm SQL}} \sim \left(\frac{L}{\Lambda} \right)^2 (\alpha L). \tag{59}$$

As the length of the first fiber must be at least a few times longer than the soliton period Λ for the adiabatic approxima-
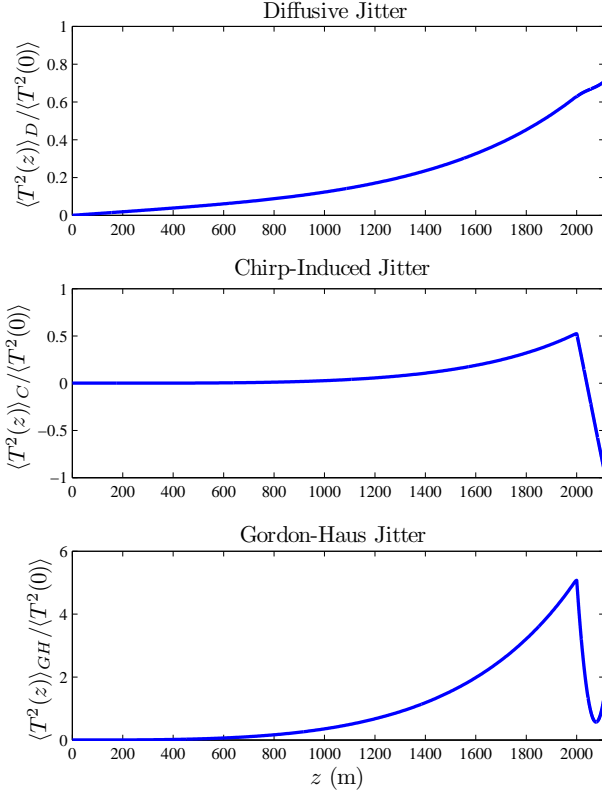
FIG. 4: (Color online) Evolution of diffusive jitter (top), chirp-induced jitter (center), and Gordon-Haus jitter (bottom). All plots are normalized with respect to the initial jitter $\langle \hat{T}^2(0) \rangle$.

tion to hold and for the bandwidth to be significantly reduced, L/Λ is approximately fixed, and the Gordon-Haus jitter can be reduced only if a figure of merit,

$$\text{FOM} \equiv \frac{1}{\alpha\Lambda} = \frac{2}{\pi}\frac{|\beta|}{\alpha\tau^2}, \qquad (60)$$

is enhanced. Since this is a rough order-of-magnitude estimate, a representative value of Λ, say at $z = L$, can be used. The figure of merit suggests that the performance of the soliton control scheme can be improved by reducing the pulse width, increasing the overall dispersion coefficient, or reducing the loss coefficient.

Reducing the pulse width is the most convenient way of obtaining better enhancement, as the adiabatic bandwidth reduction can be achieved over a shorter distance with less loss of photons. For example, using $\tau(0) = 500$ fs, $L = 1$ km, $L_\beta = 0.3$ km, $L' = 44$ m, and otherwise the same parameters as in Sec. IV B, the squeezing ratio becomes -6.0 dB, while using $\tau(0) = 200$ fs, $L = 500$ m, $L_\beta = 1/12$ km, and $L' = 16.2$ m gives a squeezing ratio of -7.3 dB. The shorter pulse width, however, significantly enhances higher-order dispersive and nonlinear effects. Raman scattering, in particular, contributes additional quantum noise because of coupling to optical phonons [22]. It is beyond the scope of this paper to investigate these higher-order effects, so a more conservative pulse width of 1 ps is used in the preceding section. A larger

overall dispersion coefficient, on the other hand, means that more photons or a higher nonlinearity are required for a soliton to form, so the Raman effect may also become more significant with a larger dispersion coefficient. The Raman effect can be reduced by cooling the fiber and reducing the number of thermal phonons [22], if it becomes a significant problem.

Further advance in optical fiber technology should be able to increase the figure of merit by reducing loss, since the specialty fibers assumed in Sec. IV B have a higher loss than usual transmission fibers by a factor of two. Using $\alpha = 0.2$ dB/km instead of 0.4 dB/km in Sec. IV B, for instance, reduces the squeezing ratio to -4.7 dB. Spectral filtering or frequency-dependent gain [23] provides another way of controlling the Gordon-Haus effect, although it adds another level of complexity to the experimental setup, and it is beyond the scope of this paper to investigate how the frequency-dependent dissipation or amplification might help the quantum enhancement scheme. Finally, the design of the setup assumed in Sec. IV B is not fully optimized, and further optimization of parameters, fiber dispersion profiles, and bandwidth narrowing strategy should be able to improve the enhancement.

V. EFFECT OF LOSS ON THE TRANSMISSION OF QUANTUM-ENHANCED TIMING INFORMATION

Provided that quantum enhancement of pulse position accuracy can be achieved, the information still needs to be transmitted through unavoidably lossy channels. It is hence an important question to ask how loss affects the quantum-enhanced information in optical information transmission systems. Equation (43) governs the general evolution of the timing jitter under the effects of loss, dispersion, and nonlinearity, but in order to estimate the relative magnitude of the decoherence effects and gain more insight into the decoherence processes, in this section Eq. (43) is explicitly solved for various systems and compared with the standard quantum limit.

A. Linear non-dispersive systems

Without dispersion, the timing jitter increases only due to the diffusive component $\langle \hat{T}^2(z) \rangle_\text{D}$. An analytic expression for $\langle \hat{T}^2(z) \rangle$ can then be derived from Eq. (43), as $\Delta t(z)$ and $\Delta\omega(z)$ remain constant,

$$\langle \hat{T}^2(z) \rangle = \langle \hat{T}^2(0) \rangle + \frac{\Delta t^2(0)}{N(z)}(1 - e^{-\alpha z}). \qquad (61)$$

If the initial variance obeys coherent-field statistics, that is, $\langle \hat{T}^2(0) \rangle = \Delta t^2(0)/N(0)$ according to Eq. (22), the subsequent jitter is

$$\langle \hat{T}^2(z) \rangle_\text{coh} = \frac{\Delta t^2(0)}{N(z)}, \qquad (62)$$

and obeys the same coherent-field statistics but for the reduced photon number $N(z)$. This is consistent with intuition. On the other hand, in the high loss limit ($\alpha z \gg 1$), the

term $\Delta t^2(0)/N(z)$ is likely to dominate over the initial jitter $\langle \hat{T}^2(0) \rangle$, so in most cases the position of a significantly attenuated pulse relaxes to coherent-field statistics independent of its initial fluctuation. This justifies the assumption in Sec. IV that a laser pulse exiting a laser cavity has such statistics, regardless of the quantum properties of the pulse inside the cavity.

Equation (61) can be renormalized as

$$R(z) \equiv \frac{\langle \hat{T}^2(z) \rangle}{\langle \hat{T}^2(z) \rangle_{\mathrm{SQL}}}$$
$$= R(0)e^{-\alpha z} + 4\Delta t^2(0)\Delta \omega^2(0)(1 - e^{-\alpha z}). \quad (63)$$

When $\langle \hat{T}^2 \rangle \ll \Delta t^2$ and $\langle \hat{\Omega}^2 \rangle \ll \Delta \omega^2$, classical theory predicts that $4\Delta t^2 \Delta \omega^2 \approx 1$. Equation (63) then suggests that the relative increase in timing jitter is independent of the initial squeezing ratio $R(0)$. This is nevertheless not true in general, as Δt may depend on both $\Delta \omega$ and R when the classical theory fails. In Appendix C, the exact dependence of Δt on $\Delta \omega$ and R is calculated for a specific multiphoton state with a Gaussian pulse shape called the jointly Guassian state. The expression $4\Delta t^2 \Delta \omega^2$ is given by

$$4\Delta t^2 \Delta \omega^2 = \frac{R}{N} + \frac{(1 - 1/N)^2}{1 - 1/(NR)}, \quad (64)$$

which results in the following exact expression for an initial jointly Gaussian state,

$$R(z) = R(0)e^{-\alpha z} + \left[\frac{R}{N} + \frac{(1 - 1/N)^2}{1 - 1/(NR)} \right]_{z=0} (1 - e^{-\alpha z}). \quad (65)$$

For a large photon number ($N \gg 1$) and moderate enhancement ($1 \geq R \gg 1/N$), $4\Delta t^2 \Delta \omega^2 \approx 1$, as classical theory would predict for a Gaussian pulse. In this regime, the quantum-enhanced information is just as sensitive to loss as standard-quantum-limited information. When R gets close to the Heisenberg limit $1/N$, however, $\Delta t \Delta \omega$ approaches infinity. This is because maximal coincident-frequency correlations are required to achieve the Heisenberg limit [1], but heuristically speaking, if the photons have exactly the same momentum, they must have infinite uncertainties in their relative positions, leading to an infinite pulse width Δt. Owing to the abrupt increase in $4\Delta t^2 \Delta \omega^2$ when R approaches $1/N$, the quantum enhancement becomes much more sensitive to loss. In the Heisenberg limit of $R \to 1/N$, $\Delta t \to \infty$, any loss completely detroys the timing accuracy and leads to an infinite jitter, according to Eq. (65).

B. Linear dispersive systems

If the system is lossy, dispersive, but linear, it is not difficult to show that

$$\Delta t^2(z) = \Delta t^2(0) + C(0) \int_0^z dz' \beta(z')$$
$$+ \Delta \omega^2(0) \left[\int_0^z dz' \beta(z') \right]^2, \quad (66)$$

$$C(z) = C(0) + 2\Delta \omega^2(0) \int_0^z dz' \beta(z'), \quad (67)$$

$$\Delta \omega^2(z) = \Delta \omega^2(0). \quad (68)$$

The following result can then be obtained from Eq. (43) after some algebra,

$$\langle \hat{T}^2(z) \rangle = \langle \hat{T}^2(0) \rangle + \langle \hat{T}(0)\hat{\Omega}(0) + \hat{\Omega}(0)\hat{T}(0) \rangle \int_0^z dz' \beta(z')$$
$$+ \langle \hat{\Omega}^2(0) \rangle \left[\int_0^z dz' \beta(z') \right]^2 + \frac{\Delta t^2(z)}{N(z)}(1 - e^{-\alpha z}). \quad (69)$$

This result is similar to that in the previous section, except for the presence of quantum dispersion and the dispersive spread of the pulse width $\Delta t(z)$ that leads to increased jitter. With initially coherent-field statistics, $\langle \hat{T}^2(0) \rangle$ and $\langle \hat{\Omega}^2(0) \rangle$ are given by Eqs. (22) and (20), respectively, while by similar arguments, the coherent-field statistics for $\langle \hat{T}\hat{\Omega} + \hat{\Omega}\hat{T} \rangle$ is

$$\langle \hat{T}\hat{\Omega} + \hat{\Omega}\hat{T} \rangle_{\mathrm{coh}} = \frac{C}{N}. \quad (70)$$

This leads to the following position variance for a pulse with initially coherent-field statistics,

$$\langle \hat{T}^2(z) \rangle_{\mathrm{coh}} = \frac{\Delta t^2(z)}{N(z)}, \quad (71)$$

which still maintains the coherent-field statistics for the dispersed pulse width and the reduced photon number. In the high loss limit ($\alpha z \gg 1$), the coherent-field statistics is again approached regardless of the initial conditions.

For an initial jointly Gaussian quantum state, on the other hand, the normalized version of Eq. (69) is

$$R(z) = \left[R(0) + \frac{4}{R(0)}\zeta^2 \right] e^{-\alpha z}$$
$$+ \left[4\Delta t^2(0)\Delta \omega^2(0) + 4\zeta^2 \right](1 - e^{-\alpha z}), \quad (72)$$

where ζ is the normalized effective propagation distance,

$$\zeta \equiv \Delta \omega^2(0) \int_0^z dz' \beta(z'), \quad (73)$$

and $4\Delta t^2(0)\Delta \omega^2(0)$ is given by Eq. (64) evaluated at $z = 0$. As long as the loss is moderate so that $e^{-\alpha z} \gg 1 - e^{-\alpha z}$, quantum dispersion, given by the term proportional $\zeta^2/R(0)$, becomes the dominant effect and overwhelms the initial enhancement when ζ exceeds $R(0)/2$.

If the net dispersion $\int_0^z dz' \beta(z')$ is zero, both quantum and classical dispersion are eliminated, and the jitter growth becomes identical to that in a non-dispersive and linear system given by Eq. (61).

C. Soliton-like systems

The previous sections show that coherent-field statistics is maintained in a linear system, but as Sec. IV clearly shows, non-trivial statistics can arise from the quantum dynamics of a nonlinear system. The complex evolution of $\Delta t(z)$, $C(z)$, and $\Delta\omega(z)$ in general prevents one from solving Eq. (43) explicitly, except for special cases such as solitons.

If the dispersion is constant and the pulse propagates in the fiber as a soliton, $C(z)$ is zero, while $\Delta t(z)$ and $\Delta\omega(z)$ can be regarded as constant if $\langle\hat{T}^2\rangle \ll \Delta t^2$ and $\langle\hat{\Omega}^2\rangle \ll \Delta\omega^2$ throughout propagation. Equation (43) can then be solved explicitly,

$$\langle\hat{T}^2(z)\rangle = \langle\hat{T}^2(0)\rangle + \langle\hat{\Omega}^2(0)\rangle\beta^2 z^2 + \frac{\Delta t^2(0)}{N(0)}(e^{\alpha z} - 1)$$
$$+ \frac{2\beta^2\Delta\omega^2(0)}{N(0)}\left(\frac{e^{\alpha z} - 1}{\alpha^2} - \frac{z}{\alpha} - \frac{z^2}{2}\right), \quad (74)$$

where $\langle\hat{T}(0)\hat{\Omega}(0) + \hat{\Omega}(0)\hat{T}(0)\rangle$ is assumed to be zero for simplicity. If $4\langle\hat{T}^2(0)\rangle\langle\hat{\Omega}^2(0)\rangle = (\pi^2/9)[1/N^2(0)]$ is also assumed for a soliton pulse for simplicity, Eq. (74) can be normalized to give

$$R(z) = R(0)e^{-\alpha z} + \frac{\pi^4}{81}\frac{1}{R(0)}\left(\frac{z}{\Lambda}\right)^2 e^{-\alpha z} + \frac{\pi^2}{12}\frac{\tau^2}{N(0)}(e^{\alpha z} - 1)$$
$$+ \frac{2\pi^2}{9}\frac{e^{-\alpha z}}{\Lambda^2}\left(\frac{e^{\alpha z} - 1}{\alpha^2} - \frac{z}{\alpha} - \frac{z^2}{2}\right). \quad (75)$$

In the low loss regime with $\alpha\Lambda \ll 1$ and $\alpha z \ll 1$, Eq. (75) can be further simplified,

$$R(z) \approx R(0) + \frac{\pi^4}{81}\frac{1}{R(0)}\left(\frac{z}{\Lambda}\right)^2 + \frac{\pi^2}{12}\frac{\tau^2}{N(0)}(\alpha z)$$
$$+ \frac{\pi^2}{27}\left(\frac{z}{\Lambda}\right)^2(\alpha z). \quad (76)$$

Quantum dispersion is again the dominant effect in this regime, while decoherence effects are much smaller, by a factor of αz approximately.

Even if the net dispersion is zero and quantum dispersion is compensated, the Gordon-Haus effect cannot be completely eliminated by dispersion management in the presence of non-linearity and may become significant, as the numerical analysis in Sec. IV B shows. An order-of-magnitude estimate of Gordon-Haus jitter can be performed by considering soliton propagation in a constant negative dispersion fiber, just as in the previous case, followed by a dispersion-compensating fiber of length L' with positive dispersion coefficient β'. If L' is short, the effective nonlinearity experienced by the pulse in the second fiber can be neglected, and $\Delta\omega(z)$ can be regarded as constant. Assuming that $\beta L + \beta' L' = 0$, the integral in Eq. (46) can be solved to give the Gordon-Haus jitter,

$$\langle\hat{T}^2(L+L')\rangle_{\mathrm{GH}} \approx \frac{\alpha\Delta\omega^2(0)}{6N(0)}\beta^2 L^2(L+L')$$
$$\approx \frac{\alpha\Delta\omega^2(0)}{6N(0)}\beta^2 L^3. \quad (77)$$

The normalized contribution to the squeezing ratio is therefore

$$\frac{\langle\hat{T}^2(L+L')\rangle_{\mathrm{GH}}}{\langle\hat{T}^2(L+L')\rangle_{\mathrm{SQL}}} \approx \frac{\pi^2}{54}\left(\frac{L}{\Lambda}\right)^2(\alpha L). \quad (78)$$

Compared with the Gordon-Haus jitter at the end of the first fiber given by the last term of Eq. (76), dispersion management cuts the jitter by half, but the expression maintains its functional dependence on the parameters of the first fiber. This estimate also justifies the use of Eq. (59) to estimate the Gordon-Haus jitter at the end of the two fibers in Sec. IV C. To minimize the impact of Gordon-Haus jitter on the quantum-enhanced timing accuracy in a dispersion-managed soliton system, the condition

$$L^3 \ll \frac{54}{\pi^2}\left(\frac{\Lambda^2}{\alpha}\right)R \quad (79)$$

is required.

VI. CONCLUSION

In conclusion, the decoherence effect by optical loss on adiabatic soliton control and on the transmission of quantum-enhanced timing information has been extensively studied. It is found that an appreciable enhancement can still be achieved by the soliton scheme using current technology, despite an increase of timing jitter due to the presence of loss. It is also found that the quantum-enhanced timing accuracy should be much lower than the Heisenberg-limited accuracy to avoid increased sensitivity to photon loss during transmission, and the net dispersion in the transmission system should be minimized in order to reduce quantum dispersion and the Gordon-Haus effect.

Although the most important pulse propagation effects have been considered in this analysis, higher-order effects, such as third-order dispersion, self-steepening, and Raman scattering [14] might provide further adverse impact on the quantum enhancement if the optical pulse is ultrashort. In particular, the inelastic Raman scattering process is expected to be a significant source of decoherence for ultrashort pulses [22]. It is beyond the scope of this paper to investigate these higher-order effects, but they should be of minor importance for picosecond pulses and the propagation distances considered in this paper.

Finally, it is worth noting that while this paper focuses on optical pulses, the developed formalism is equally valid for describing the transverse position and momentum of optical beams [24] and the center-of-mass variables of Bose-Einstein condensates [9]. Decoherence by loss of particles in those systems can be studied using the formalism developed in this paper and parameters specific to those systems.

APPENDIX A: DERIVATION OF EXACT HEISENBERG LIMITS

An exact Heisenberg limit can be derived if the inverse photon-number operator $\hat{N}^{-1}$ is used instead of $1/N$ in the definitions of $\hat{T}$, $\hat{\Omega}$, Δt, and $\Delta \omega$ in Eqs. (9), (11), (14), and (15), just as in Refs. [9] and [10],

$$\hat{T}' \equiv \hat{N}^{-1} \int dt\, t \hat{A}^\dagger \hat{A}, \tag{A1}$$

$$\hat{\Omega}' \equiv \hat{N}^{-1} \int d\omega\, \omega \hat{a}^\dagger \hat{a}, \tag{A2}$$

$$\Delta t' \equiv \left\langle \hat{N}^{-1} \int dt\, t^2 \hat{A}^\dagger \hat{A} \right\rangle^{1/2}, \tag{A3}$$

$$\Delta \omega' \equiv \left\langle \hat{N}^{-1} \int d\omega\, \omega^2 \hat{a}^\dagger \hat{a} \right\rangle^{1/2}. \tag{A4}$$

These operators are well defined as long as the quantum state has zero vacuum-state component ($\langle 0|\hat{\rho}|0\rangle = 0$). Starting from the Heisenberg uncertainty principle for $\hat{T}'$ and $\hat{\Omega}'$,

$$\langle \hat{T}'^2 \rangle \langle \hat{\Omega}'^2 \rangle \geq \frac{\langle \hat{N}^{-2} \rangle}{4}, \tag{A5}$$

and the inequality

$$\left\langle \hat{N}^{-2} \int d\omega \int d\omega'\, (\omega - \omega')^2 \hat{a}^\dagger \hat{a}'^\dagger \hat{a} \hat{a}' \right\rangle \geq 0, \tag{A6}$$

one can obtain the exact inequality

$$\langle \hat{\Omega}'^2 \rangle \leq \Delta \omega'^2, \tag{A7}$$

and the exact Heisenberg limit for the new position operator,

$$\langle \hat{T}'^2 \rangle_{\mathrm{H}} = \frac{\langle \hat{N}^{-2} \rangle}{4 \Delta \omega'^2}. \tag{A8}$$

The difference between Eqs. (28) and (A8) is negligible for small photon-number fluctuations. The exact Heisenberg limit on $\langle \hat{\Omega}'^2 \rangle$ is similar.

APPENDIX B: NOISE STATISTICS

In this section the expression $\langle \hat{S}_T(z) \hat{S}_T(z') \rangle$ in Eq. (38) is calculated. The derivations of $\langle \hat{S}_\Omega(z) \hat{S}_\Omega(z') \rangle$ in Eq. (39) and $\langle \hat{S}_T(z) \hat{S}_\Omega(z') + \hat{S}_\Omega(z) \hat{S}_T(z') \rangle$ in Eq. (40) are similar. Substituting Eq. (35) into Eq. (38) gives

$$\langle \hat{S}_T(z) \hat{S}_T(z') \rangle = \frac{1}{NN'} \int dt \int dt'\, tt' \Big[\langle \hat{s}^\dagger \hat{A} \hat{s}'^\dagger \hat{A}' \rangle + \langle \hat{s}^\dagger \hat{A} \hat{A}'^\dagger \hat{s}' \rangle$$
$$+ \langle \hat{A}^\dagger \hat{s} \hat{A}'^\dagger \hat{s}' \rangle + \langle \hat{A}^\dagger \hat{s} \hat{s}'^\dagger \hat{A}' \rangle \Big], \tag{B1}$$

where $N = N(z)$, $N' = N(z')$, $\hat{s} = \hat{s}(z,t)$, $\hat{A} = \hat{A}(z,t)$, $\hat{s}' = \hat{s}(z',t')$, and $\hat{A}' = \hat{A}(z',t')$. If the noise reservoir is in the vacuum state, $\hat{s}|0_{\mathrm{reservoir}}\rangle = \langle 0_{\mathrm{reservoir}}|\hat{s}^\dagger = 0$, so only the last term in Eq. (B1) is non-zero,

$$\langle \hat{S}_T(z) \hat{S}_T(z') \rangle = \frac{1}{NN'} \int dt \int dt'\, tt' \langle \hat{A}^\dagger \hat{s} \hat{s}'^\dagger \hat{A}' \rangle$$
$$= \frac{1}{NN'} \int dt \int dt'\, tt'$$
$$\times \left[\langle \hat{A}^\dagger \hat{A}' \rangle \alpha \delta(z - z') \delta(t - t') + \langle \hat{A}^\dagger \hat{s}'^\dagger \hat{s} \hat{A}' \rangle \right]$$
$$= \frac{\alpha \Delta t^2}{N} \delta(z - z')$$
$$+ \frac{1}{NN'} \int dt \int dt'\, tt' \langle \hat{A}^\dagger \hat{s}'^\dagger \hat{s} \hat{A}' \rangle. \tag{B2}$$

The first term on the right-hand side of Eq. (B2) is the desired result, while the second term can be rewritten as

$$\frac{1}{NN'} \int dt \int dt'\, tt' \langle \hat{A}^\dagger \hat{s}'^\dagger \hat{s} \hat{A}' \rangle$$
$$= \frac{1}{NN'} \int dt \int dt'\, tt' \langle [\hat{A}^\dagger, \hat{s}'^\dagger][\hat{s}, \hat{A}'] \rangle. \tag{B3}$$

If the system is linear, the commutator between $\hat{s}$ and $\hat{A}$ is always zero [13], but because $\hat{s}$ does not commute with $\hat{A}^\dagger$ and $\hat{A}$ is coupled to $\hat{A}^\dagger$ by the nonlinear term in Eq. (31), $\hat{s}$ may fail to commute with $\hat{A}$. That said, it can be argued that the optical field operator must always commute with future noise operators due to causality and the infinitesimally short memory of $\hat{s}$,

$$[\hat{A}^\dagger, \hat{s}'^\dagger] = 0 \text{ if } z < z', \tag{B4}$$
$$[\hat{s}, \hat{A}'] = 0 \text{ if } z > z', \tag{B5}$$

so Eq. (B3) can be non-zero only at $z = z'$. The commutator between $\hat{s}$ and $\hat{A}$ at $z = z'$ due to the parametric coupling of $\hat{A}$ and $\hat{A}^\dagger$ can be estimated by a perturbative technique. Consider an integral form of Eq. (31) with the nonlinear term and the Langevin noise term only,

$$\hat{A}(z + \Delta z) = \hat{A}(z) + \int_z^{z+\Delta z} dz' \left[i\kappa \hat{A}^\dagger(z') \hat{A}(z') \hat{A}(z') + \hat{s}(z') \right], \tag{B6}$$

and $\hat{A}^\dagger(z')$ given by the Hermitian conjugate of Eq. (B6),

$$\hat{A}^\dagger(z') = \hat{A}^\dagger(z) + \int_z^{z'} dz'' \left[-i\kappa \hat{A}^\dagger(z'') \hat{A}^\dagger(z'') \hat{A}(z'') + \hat{s}^\dagger(z'') \right]. \tag{B7}$$

The commutator between $\hat{s}$ and $\hat{A}$ at $z + \Delta z$ becomes

$$[\hat{s}(z + \Delta z), \hat{A}(z + \Delta z)]$$
$$= i\kappa \int_z^{z+\Delta z} dz' \left[\hat{s}(z + \Delta z), \hat{A}^\dagger(z') \right] \hat{A}(z') \hat{A}(z'). \tag{B8}$$

$\hat{s}(z+\Delta z)$ commutes with $\hat{A}(z')$ because $z+\Delta z > z'$, while it fails to commute with $\hat{A}^\dagger(z')$ because $\hat{A}^\dagger(z')$ given by Eq. (B7) depends explicitly on $\hat{s}^\dagger$. Thus, in the leading order of Δz,

$$[\hat{s}(z+\Delta z),\hat{A}(z+\Delta z)]$$

$$\approx i\kappa \int_z^{z+\Delta z} dz' \int_z^{z'} dz'' \left[\hat{s}(z+\Delta z),\hat{s}^\dagger(z'')\right]\hat{A}(z')\hat{A}(z'), \quad (B9)$$

which approaches 0 in the limit of $\Delta z \to 0$. Hence $\hat{s}$ commutes with $\hat{A}$ at $z = z'$, and the position noise is given only by the first term on the right-hand side of Eq. (B2), resulting in Eq. (38).

APPENDIX C: THE JOINTLY GAUSSIAN STATE

A Fock state can be expressed as [13, 25]

$$|N\rangle = \int d\omega_1 \dots \int d\omega_N \, \phi(\omega_1,\dots,\omega_N)|\omega_1,\dots,\omega_N\rangle,$$

$$= \int dt_1 \dots \int dt_N \, \psi(t_1,\dots,t_N)|t_1,\dots,t_N\rangle, \quad (C1)$$

where the spectral and temporal eigenstates are given by

$$|\omega_1,\dots,\omega_N\rangle \equiv \frac{1}{\sqrt{N!}}\hat{a}^\dagger(\omega_1)\dots\hat{a}^\dagger(\omega_N)|0\rangle, \quad (C2)$$

$$|t_1,\dots,t_N\rangle \equiv \frac{1}{\sqrt{N!}}\hat{A}^\dagger(t_1)\dots\hat{A}^\dagger(t_N)|0\rangle. \quad (C3)$$

Theses states are eigenstates of the following operators relevant to our purpose,

$$\hat{\Omega}|\omega_1,\dots,\omega_N\rangle = \left(\frac{1}{N}\sum_{n=1}^N \omega_n\right)|\omega_1,\dots,\omega_N\rangle, \quad (C4)$$

$$\hat{T}|t_1,\dots,t_N\rangle = \left(\frac{1}{N}\sum_{n=1}^N t_n\right)|t_1,\dots,t_N\rangle, \quad (C5)$$

$$\frac{1}{N}\int d\omega \, \omega^2 \hat{a}^\dagger \hat{a}|\omega_1,\dots,\omega_N\rangle = \left(\frac{1}{N}\sum_{n=1}^N \omega_n^2\right)|\omega_1,\dots,\omega_N\rangle, \quad (C6)$$

$$\frac{1}{N}\int dt \, t^2 \hat{A}^\dagger \hat{A}|t_1,\dots,t_N\rangle = \left(\frac{1}{N}\sum_{n=1}^N t_n^2\right)|t_1,\dots,t_N\rangle. \quad (C7)$$

$\phi(\omega_1,\dots,\omega_N)$ is the spectral multiphoton probability amplitude, and it is related to the temporal probability amplitude $\psi(t_1,\dots,t_N)$ by the N-dimensional Fourier transform in the slowly-varying envelope regime. Both amplitudes should also satisfy normalization and boson symmetry. To study temporal quantum enhancement, it is convenient to define the probability amplitude as a jointly Gaussian function [25],

$$\phi(\omega_1,\dots,\omega_N) = C\exp\left[-\frac{1}{4B^2}\left(\frac{1}{N}\sum_{n=1}^N \omega_n\right)^2\right.$$

$$\left. -\frac{1}{4b^2}\sum_{n=1}^N\left(\omega_n - \frac{1}{N}\sum_{m=1}^N \omega_m\right)^2\right], \quad (C8)$$

$$\psi(t_1,\dots,t_N) = C'\exp\left[-N^2B^2\left(\frac{1}{N}\sum_{n=1}^N t_n\right)^2\right.$$

$$\left. -b^2\sum_{n=1}^N\left(t_n - \frac{1}{N}\sum_{m=1}^N t_m\right)^2\right], \quad (C9)$$

where B and b are arbitrary and real constants, and C and C' are normalization constants. Explicit expressions for $\langle\hat{\Omega}^2\rangle$, $\langle\hat{T}^2\rangle$, $\Delta\omega^2$, and Δt^2 can be obtained using Eqs. (C4)-(C7) and Appendix B of Ref. [25],

$$\langle\hat{\Omega}^2\rangle = B^2, \quad (C10)$$

$$\langle\hat{T}^2\rangle = \frac{1}{4N^2B^2}, \quad (C11)$$

$$\Delta\omega^2 = B^2 + \left(1-\frac{1}{N}\right)b^2, \quad (C12)$$

$$\Delta t^2 = \frac{1}{4N^2B^2} + \left(1-\frac{1}{N}\right)\frac{1}{4b^2}. \quad (C13)$$

In the limit of $b \to 0$, $\langle\hat{T}^2\rangle$ reaches the Heisenberg limit,

$$\langle\hat{T}^2\rangle = \frac{1}{4N^2\Delta\omega^2}, \quad (C14)$$

and the quantum state can be written as a state of photons with maximal coincident-frequency correlations,

$$|N\rangle \propto \int d\omega \, \exp\left(-\frac{\omega^2}{4B^2}\right)|\omega,\dots,\omega\rangle. \quad (C15)$$

On the other hand, when $B^2 = b^2/N$, $\langle\hat{T}^2\rangle$ is at the standard quantum limit,

$$\langle\hat{T}^2\rangle = \frac{1}{4N\Delta\omega^2}, \quad (C16)$$

the quantum state has only one excited Gaussian mode [25],

$$|N\rangle \propto \int d\omega_1 \dots \int d\omega_N \prod_{n=1}^N \exp\left(-\frac{\omega_n}{4b^2}\right)|\omega_1,\dots,\omega_N\rangle$$

$$\propto \left[\int d\omega \, \exp\left(-\frac{\omega}{4b^2}\right)\hat{a}^\dagger(\omega)\right]^N|0\rangle, \quad (C17)$$

and therefore also satisfies the coherent-field statistics [12, 13]. These limits and the corresponding quantum states are consistent with those suggested in Ref. [1]. With Eqs. (C12) and (C13), the pulse width Δt can be determined explicitly in terms of $\Delta\omega$ and the squeezing ratio $R = \Delta\omega^2/(NB^2)$,

$$\Delta t^2 = \frac{1}{4\Delta\omega^2}\left[\frac{R}{N} + \frac{(1-1/N)^2}{1-1/(NR)}\right]. \quad (C18)$$

[1] V. Giovannetti, S. Lloyd, and L. Maccone, Nature (London) **412**, 417 (2001); V. Giovannetti, S. Lloyd, and L. Maccone, Phys. Rev. A **65**, 022309 (2002).

[2] V. Giovannetti, L. Maccone, J. H. Shapiro, and F. N. C. Wong, Phys. Rev. Lett. **88**, 183602 (2002); O. Kuzucu, M. Fiorentino, M. A. Albota, F. N. C. Wong, and F. X. Kärtner, Phys. Rev. Lett. **94**, 083601 (2005).

[3] M. Tsang, Phys. Rev. Lett. **97**, 023902 (2006).

[4] V. Giovannetti, S. Lloyd, and L. Maccone, Phys. Rev. Lett. **96**, 010401 (2006); V. Giovannetti, S. Lloyd, and L. Maccone, Science **306**, 1330 (2004).

[5] S. J. Carter, P. D. Drummond, M. D. Reid, and R. M. Shelby, Phys. Rev. Lett. **58**, 1841 (1987); P. D. Drummond and S. J. Carter, J. Opt. Soc. Am. B **4**, 1565 (1987); M. J. Potasek and B. Yurke, Phys. Rev. A **35**, 3974 (1987); M. J. Potasek and B. Yurke, *ibid.* **38**, 1335 (1988); H. A. Haus, *Electromagnetic Noise and Quantum Optical Measurements* (Springer, Berlin, 2000).

[6] J. M. Fini and P. L. Hagelstein, Phys. Rev. A **66**, 033818 (2002).

[7] P. L. Hagelstein, Phys. Rev. A **54**, 2426 (1996); J. M. Fini, P. L. Hagelstein, and H. A. Haus, *ibid.* **60**, 2442 (1999).

[8] B. Huttner and S. M. Barnett, Phys. Rev. A **46**, 4306 (1992); R. Matloob, R. Loudon, S. M. Barnett, and J. Jeffers, *ibid.* **52**, 4823 (1995).

[9] T. Vaughan, P. Drummond, and G. Leuchs, Phys. Rev. A **75**, 033617 (2007).

[10] Y. Lai and H. A. Haus, Phys. Rev. A **40**, 844 (1989).

[11] H. A. Haus and Y. Lai, J. Opt. Soc. Am. B **7**, 386 (1990).

[12] U. M. Titulaer and R. J. Glauber, Phys. Rev. **140**, 676 (1965); U. M. Titulaer and R. J. Glauber, *ibid.* **145** 1041 (1966).

[13] L. Mandel and E. Wolf, *Optical Coherence and Quantum Optics* (Cambridge University Press, Cambridge, 1995).

[14] G. P. Agrawal, *Nonlinear Fiber Optics* (Academic Press, San Diego, 2001).

[15] H. A. Haus, J. Opt. Soc. Am. B **8**, 1122 (1991).

[16] Y. Lai and H. A. Haus, Phys. Rev. A **40**, 854 (1989).

[17] J. P. Gordon and H. A. Haus, Opt. Lett. **11**, 665 (1986).

[18] H. H. Kuehl, Opt. Lett. **5**, 709 (1988).

[19] V. A. Bogatyrev, M. M. Bubnov, E. M. Dianov, A. S. Kurkov, P. V. Mamyshev, A. M. Prokhorov, S. D. Rumyantsev, V. A. Semenov, S. L. Semenov, A. A. Sysoliatin, S. V. Chernikov, A. N. Gur'yanov, G. G. Devyatykh, and S. I. Miroshnichenko, J. Lightwave Technol. **9**, 561 (1991).

[20] L. Grüner-Nielsen, M. Wandel, P. Kristensen, C. Jørgensen, L. V. Jørgensen, B. Edvold, B. Pálsdóttir, and D. Jakobsen, J. Lightwave Technol. **23**, 3566 (2005).

[21] N. J. Smith, W. Forysiak, and N. J. Doran, Electron. Lett. **32**, 2085 (1996).

[22] F. X. Kärtner, D. J. Dougherty, H. A. Haus, and E. P. Ippen, J. Opt. Soc. Am. B **11**, 1267 (1994); J. F. Corney and P. D. Drummond, *ibid.* **18**, 153 (2001).

[23] A. Mecozzi, J. D. Moores, H. A. Haus, and Y. Lai, Opt. Lett. **16**, 1841 (1991); Y. Kodama and A. Hasegawa, Opt. Lett. **17**, 31 (1992).

[24] S. M. Barnett, C. Fabre, and A. Maître, Eur. Phys. J. D **22**, 513 (2003); N. Treps, U. Andersen, B. Buchler, P. K. Lam, A. Maître, H.-A. Bachor, and C. Fabre, Phys. Rev. Lett. **88**, 203601 (2002); N. Treps, N. Grosse, W. P. Bowen, C. Fabre, H.-A. Bachor, P. K. Lam, Science **301**, 940 (2003).

[25] M. Tsang, "Relationship between resolution enhancement and multiphoton absorption rate in quantum lithography," e-print quant-ph/0607114 (to appear in Phys. Rev. A).